RESISTANCE OF A DRILLED SHAFT FOOTING TO OVERTURNING LOADS, MODEL TESTS AND CORRELATION WITH THEORY

By

Don L. Ivey,

Kenneth J. Koch

and

Carl F. Raba, Jr.

Research Report Number 105-2

Design of Footings for Minor Service Structures

Research Study Number 2-5-67-105

Sponsored by

The Texas Highway Department

in cooperation with the

Department of Transportation, Federal Highway Administration,

Bureau of Public Roads

July, 1968

TEXAS TRANSPORTATION INSTITUTE

Texas A&M University

College Station, Texas

ACKNOWLEDGEMENTS

This research was conducted under an interagency contract between the Texas Transportation Institute and the Texas Highway Department. It was sponsored jointly by the Texas Highway Department and the Bureau of Public Roads. Liason was maintained through Mr. D. L. Hawkins and Mr. H. D. Butler, contact representatives for the Texas Highway Department, and through Mr. Robert J. Prochaska of the Bureau of Public Roads.

The theory presented in Research Report 105-1 was programmed for the IBM 7094 for analysis of the footings in this study by Mr. Leon E. Travis, III, and Mr. Kurt A. Schember.

The opinions, findings, and conclusions expressed in this publication are those of the authors and not necessarily those of the Bureau of Public Roads.

SYNOPSIS

Reported in this paper are the results of twenty-eight model tests of drilled shaft footings subjected to overturning horizontal loads. The models are geometrically similar but reduced by a factor of six compared to the average size of footings used for minor service structures in Texas. The soils investigated range from cohesionless sands, through soils with both cohesion and an angle of shear resistance, to clays with no angle of shear resistance when tested using the unconsolidated-undrained quick triaxial compression test.

The results of the model footing tests are compared with the theory developed in this study.[1*] It was found that the conventional methods of predicting ultimate load were conservative by as much as 500% for the cohesionless sands and by as little as 20% for the clays. The coefficients developed in the new theoretical treatment are evaluated so that the ultimate loads on this type of footing in any given soil can be predicted.

*Refers to numbers in selected references.

TABLE OF CONTENTS

Pages

INTRODUCTION 7

EQUIPMENT AND INSTRUMENTATION 7
- General
- Loading System
- Load Measurement
- Rotation Measurement

PLACEMENT OF FOOTINGS AND SOIL CONDITIONS 8
- Easterwood Clay
- Trinity Clay
- Laboratory Sandy Clay
- Ottawa Sand

TESTING PROCEDURE 10

TESTING RESULTS 11

COMPARISON OF TEST RESULTS AND THEORY 13

SUMMARY 17

SELECTED REFERENCES 17

APPENDIX 18

NOTATION

c = cohesion (force/length^2).*

ϕ = angle of shear resistance (degrees).

γ = unit weight, in place or wet (force/length^3).

γ_1 = modified unit weight of soil in the direction of the applied load (force/length^3).

γ_2 = modified unit weight of soil in the direction opposite the applied load (force/length^3).

P = horizontal load applied to footing at some distance H above ground (force).

H = height of horizontal load, P, above ground (length).

D = depth of footing (length).

d = footing diameter (length).

a = depth to point of footing rotation (length).

K_0 = coefficient of earth pressure at rest (dimensionless).

K_1 = coefficient of passive earth pressure applied to unit weight term (dimensionless).

K_2 = coefficient of passive earth pressure applied to cohesion term (dimensionless).

K_3 = coefficient of active earth pressure (dimensionless).

k = unit weight coefficient (dimensionless).

J_1 = coefficient of shear stress, vertical footing surfaces (dimensionless).

J_2 = coefficient of shear stress, footing bottom (dimensionless).

B = earth pressure coefficient modifier (dimensionless).

*The dimensions of the various symbols are given in parentheses after each definition.

Introduction

The wide use of drilled shaft footings to support service structures necessary for the functioning of a highway system has focused attention on the highly conservative design procedures presently in use. The foundations of structures such as signboards, strain poles, and lighting poles should be designed using factors of safety consistent with the relative importance of the particular structure.

As the next necessary step, after the development of a theoretical treatment for this type of foundation, a series of model tests was undertaken. The purpose of these tests was to evaluate certain coefficients introduced in the theoretical treatment and to establish the degree of precision to be expected in predicting ultimate loads with the new theoretical treatment. The footings tested ranged in diameter from 2 to 4 in., and in depth from 10 to 12 in. Height of load application ranged from 0 to 42 in. The soils in which footings were tested ranged from a dry sand with no cohesion to a clay with no angle of shear resistance. The soils are referred to in this way on the basis of the unconsolidated-undrained quick triaxial compression test. This type of test was used to determine the pertinent soil parameters because it best simulated conditions of short term loading in the field. It is recognized that the same soils tested in another way would exhibit different properties. Eight tests of footings in soils with both cohesion and an angle of shear resistance are reported.

This is the second of a series of papers to be written concerned with the design of these footings. The first, Research Report 105-1, reported in detail the theoretical development of the load prediction equations which are compared with test data in this paper.

Equipment and Instrumentation

General

In order to conduct these tests, it was necessary to develop systems capable of (1) applying a horizontal force on the footing at a uniform displacement rate and (2) measuring the load acting on the footing at known angles of rotation.

Loading System

A mechanically driven loading machine normally used for compression testing was modified to apply the overturning force to the footings. Figure 1 illustrates the loading system used for these tests. The loading machine was run at a speed of 0.05 inch per minute but the pulley system increased this speed to 0.20 inch per minute at the footing.

Load Measurement

The load applied to the footing was measured by means of a force transducer spliced into the cable approximately 2 feet from the footing. Because of the wide range of load developed, 3 transducers were used for the various tests. The capacities of each transducer were 0 to 50 pounds, 0 to 400 pounds, and 0 to 1000 pounds, respectively.

The transducers were constructed of a metal bar instrumented with a full bridge of foil strain gages.

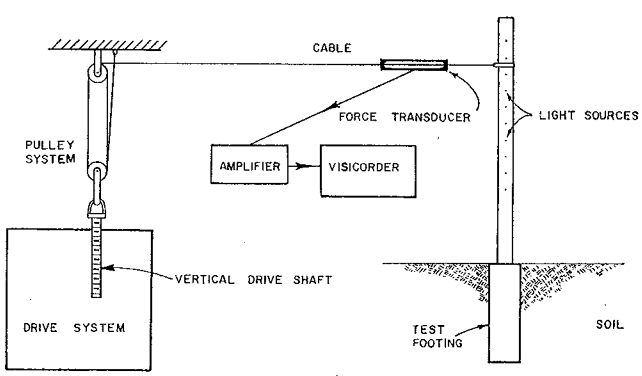

Figure 1. Loading system.

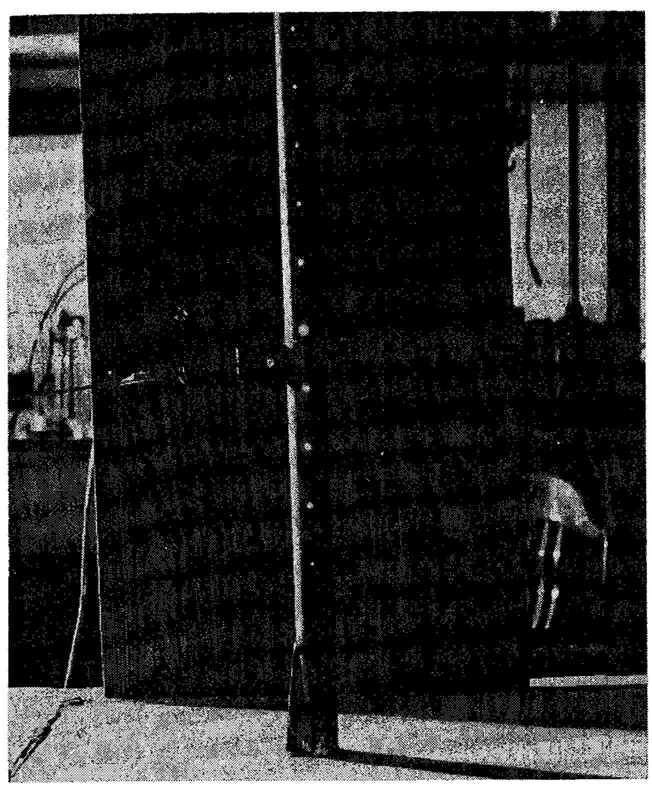

Figure 2. Point source of light.

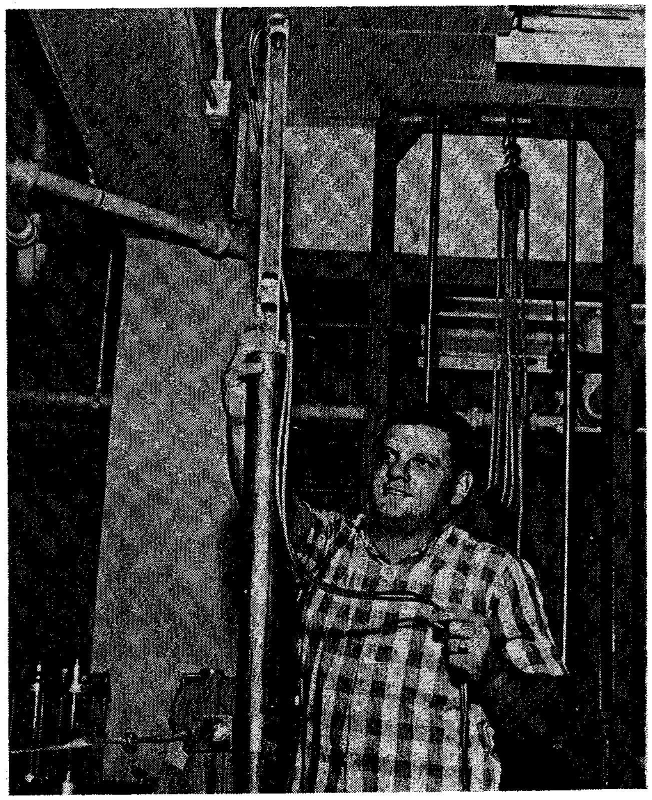

Figure 3. Placement of ultraviolet lamps.

The output voltages from these strain gages were amplified and recorded on a visicorder, providing a continuous record of the load on the footing.

Rotation Measurement

The position of the footing at known loads was measured by recording the rotation of a metal pipe that was attached to the top of each footing. The pipe was screwed onto a ¾-inch diameter threaded rod extending from the top of the concrete footings. The cable from the loading machine was connected to the pipe by means of a clamp that permitted the height of pull to be varied along the entire length of the pole.

Very small holes were drilled in the pipe on 5-inch centers along a straight line on the upper three feet of the pipe. These holes provided point sources of light from two ultraviolet lamps mounted on a carriage that had been lowered into the pipe as shown in Figures 2 and 3. As the footing was rotated, these light sources developed lines of movement on light sensitive paper mounted on a wooden panel adjacent to the pipe. The lights were turned on and off at specific loads so that the position of all ten traces could be related. A straight line was extrapolated through each series of termination points to find the position of the footing at that specific load. Because of the use of the light sensitive paper, it was necessary to perform all the tests in the dark. When the light sources were turned off, an external triggering device simultaneously marked the visicorder load record to denote the load at which the rotations were measured.

Placement of Footings and Soil Conditions

Easterwood Clay

A series of tests was conducted in the shallow sandy clay located in the vicinity of Easterwood Airport, College Station, Texas. This soil was chosen as a representative of soils possessing both cohesion (c) and an angle of shear resistance (ϕ), as determined by the unconsolidated-undrained quick triaxial test. After the test site location was determined by means of a series of auger borings, the area was leveled and prepared for the installation of footings.

A detailed procedure was established in order to install the footings as they would be placed in actual practice. Special hand augers were designed and constructed to drill the footing holes. These augers were aligned and guided during the drilled operation by a wooden template placed on top of the ground. The excavated hole was a right circular cylinder. A heavily reinforced steel cage was lowered into each hole which was subsequently filled with a cement mortar made from Type III cement and 20-30 Ottawa sand. The steel cage was vibrated with a portable vibrator to eliminate air bubbles or voids on the footing surface.

After the footing tests were completed, a total of nine borings were made with continuous sampling to a depth of 18 in. Undisturbed soil samples were obtained in the test area by a truck-mounted rotary drill rig. The specimens (2.8 in. in diameter) were sampled with thin-walled Shelby tubes. After extrusion the samples were wrapped in aluminum foil and placed in cartons for transportation back to the University's soil laboratory. Upon reaching the laboratory, the specimens were sealed with a microvan wax and stored in a humid room for classification and strength tests.

Comprehensive classification and strength tests were conducted on the soil samples. The classification tests included hydrometer analysis and determination of the Atterberg Indices; the procedures outlined by Lambe[2] were followed in these tests. The soil was classified as a CH material by the Unified Soil Classification System. A series of unconfined compression and quick triaxial tests[3] was performed to establish the soil strength parameters (cohesion and angle of shear resistance) under simulated field conditions. These tests were performed on representative samples from zero to 6 in., 6 in. to 12 in., and 12 in. to 18 in. depths.

Mohr-Coulomb failure envelopes were constructed from unconfined compression and quick triaxial compression test results on selected specimens. The average values determined for cohesion and angle of shear resistance from these tests were 2810 psf and 9° respectively. The average in place density was 133 pcf.

Trinity Clay

A series of tests was conducted in the laboratory using a soil exhibiting no angle of shear resistance in the quick triaxial tests. The clay was obtained in dry powdered form in 25 lb. bags, and mixed with water in a counter current mixer to obtain a water content of 18%. The soil was classified as a CL material by the Unified Soil Classification System.

A test bin was constructed in the Civil Engineering Department's Soil Mechanics Laboratory to facilitate these tests. The bin, 17.5 in. tall and 27.5 in. wide, was separated into 3 equal parts, each 48 in. long. The bin had a metal liner surrounded by 6 inches of concrete for rigidity. The clay was placed in 4 in. thick, loose layers and compacted with a pneumatic hammer as shown in Figure 4. The bin was completely filled with the compacted soil. A constant amount of compaction effort was applied to each layer in order to develop uniformity of unit weight and shear strength.

After the compaction of each bin was completed, holes were drilled and footings were installed as described in the Easterwood Clay section. This is shown in Figure 5.

The entire bin was covered with a sheet of thin plastic to form an airtight fit. This prevented the soil-water mixture from losing moisture through evaporation. A minimum of 14 days was allowed to elapse before the footings were tested to provide sufficient time for the mortar to cure. The compacted soil also gained strength through thixotropy[3] during this time. Thixotropy can best be described as a gain in strength with time at a constant volume-water content condition. Remolded or compacted soils are known to possess distinctive stress-strain characteristics.[4,5,6] These soils will undergo large deformations prior to mobilizing their full strengths. However, if allowed to "age," they become stiffer and more closely approach the stress-strain characteristics of an undisturbed soil.

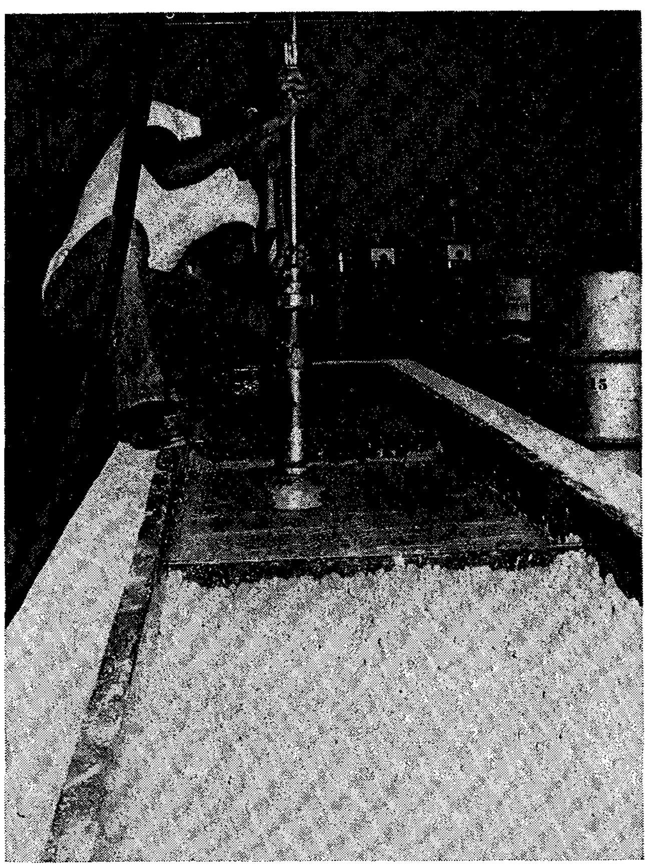

Figure 4. Compaction of clay in test bin.

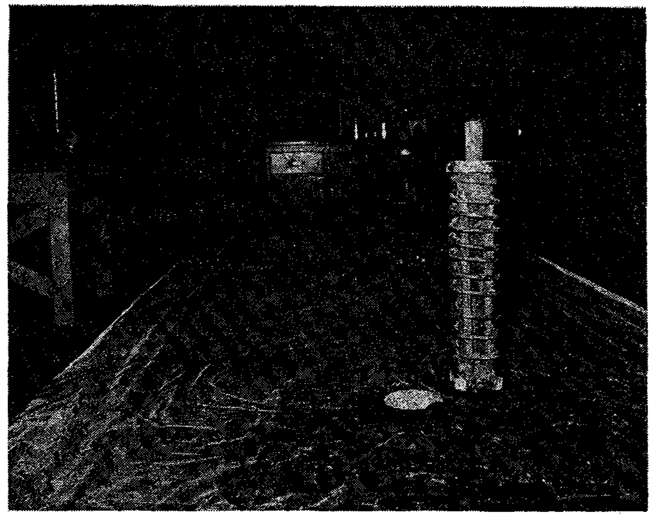

Figure 5. Footing steel reinforcement before placement of mortar.

After the footings were tested, representative samples were obtained throughout the depth of the footings in each bin. Miniature samples were obtained with a thin-walled core cutter; these samples were 1.425 in. in diameter and 3.0 in. long. The core cutter was pushed by hand into the clay and then trimmed out with a knife. The soil specimen was then extruded from the cutter, wrapped in aluminum foil, and waxed to prevent moisture loss. Quick triaxial compression tests were conducted on these specimens. The results of these tests indicated the following physical and engineering properties; cohesion (c) $=$ 3790 psf, angle of shear resistance (ϕ) $=$ 0, and unit weight in place (γ) $=$ 126 pcf.

Laboratory Sandy Clay

The sandy clay encountered in the field tests at Easterwood Airport was only representative of the higher shear strength range. Because of this, it was considered necessary to conduct additional tests in $c-\phi$ soils with lower shear strengths in order that the spectrum might be better covered.

The Trinity clay that was described previously was mixed with a locally available well-graded concrete sand in different proportions and at different water contents. The constituents of these batches are shown in Table 1:

TABLE 1

Test Number	% Sand by Weight	% Clay by Weight	Water Content (%)	In Place Unit Weight (pcf)
L-1	67	33	11.9	123
L-2	33	67	16.4	126
L-3	67	33	9.8	132

The same procedures were followed as stated previously to compact the soil, to install and test the footings, and to sample and test the sandy clay specimens.

The results of unconsolidated-undrained, quick triaxial compression tests are shown in Table 2:

TABLE 2

Batch Number	Cohesion (psf)	Angle of Internal Friction (degrees)
L-1	749	3.5
L-2	1152	5.0
L-3	1411	12.0

Ottawa Sand

A series of $c = 0$ case tests was conducted in the laboratory using 20-30 dry Ottawa sand. This material was selected as the test media because of its commercial availability and wide use as a standard research soil. The test apparatus consisted of a shallow round bin rigidly attached to the testing frame. A series of tests was conducted to establish the range of void ratios that could be achieved (loose to highly compacted) by different methods of placing the sand in the bin. These extreme conditions were represented by void ratios of 0.51 and 0.62. It was found feasible to achieve either of these extremes but very difficult to consistently produce intermediate void ratios. By testing at these extremes, the effect of void ratios on the ultimate overturning loads was indicated.

In the preparation of these tests, the precast concrete footings were suspended in place and the sand was placed around them. To achieve the loosest void ratio condition ($e = 0.62$), a "raining" technique was used to place the sand around the footing in the bin. The sand was placed in a bucket held approximately 3 in. above the surface and poured in place to a depth of 18 inches. The densest condition ($e = 0.51$) was obtained by placing the sand in the bin in 6-in. lifts and using a combination of rodding and vibration to densify it. A portable concrete vibrator was used to vibrate both the sand and the bin.

Cylindrical specimens were prepared with dry Ottawa sand at each of the two test void ratios, 0.51 and 0.62, and tested using a consolidated-drained triaxial compression test. The weight of sand was computed to fill a right circular cylinder 2.80 in. in diameter and 6.0 in. tall so as to achieve a desired void ratio. Mohr-Coulomb failure envelopes were prepared from the results of triaxial compression tests on dry sand specimens and the angles of shear resistance were determined. The sand specimens prepared at initial void ratios of 0.51 and 0.62 possessed angles of shear resistance of 37° and 32°, respectively. The in situ unit weights were 109 pcf for the void ratio of 0.51 and 102 pcf for the void ratio of 0.62.

Testing Procedure

The testing procedure used on all tests is summarized in the following paragraph.

The cable from the loading machine was secured to the pipe at the specific height of pull that had been predetermined for the particular test. The slack in the loading cable was taken up in the pulley system and the loading frame was adjusted to insure a horizontal pull. Care was taken to apply only a minimum load to the pipe. The ultraviolet lamps were then turned on briefly to mark the initial position of the footing prior to the test. The loading machine and visicorder were turned on and load was applied to the footing. The application of load to the footing was recorded on the visicorder and, as the pole rotated, the lamps inside the pipe were turned on at intervals to mark its position. This procedure was continued throughout the test. Most tests were terminated after about 20 degrees of rotation. The intersection of consecutive position lines gave an estimate of the footing rotation point as shown in Figure 6.

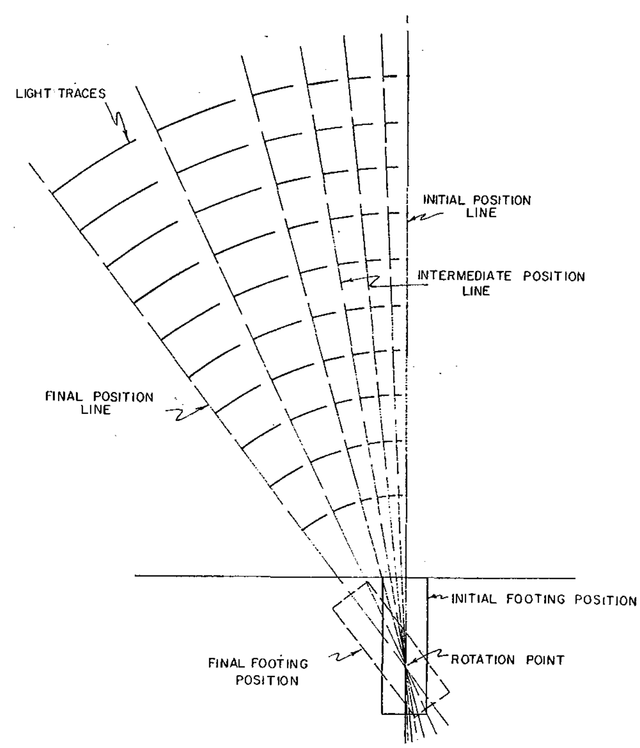

Figure 6. Displacement traces.

Test Results

The results of the model footing are presented in Table 3. Both the maximum load resisted and the load resisted after a rotation of 5° are given. In general, the maximum load occurred at a rotation slightly greater than 5°, but there were a few tests in the Ottawa sand where the maximum load occurred slightly before the 5° rotation was achieved.

Graphs of load and rotation point versus rotation (angle of deflection) are given for each test in the appendix. Typical test graphs for the footing in different materials are shown in Figures 7 through 10. In the tests in sands and clays, Figures 7 and 8, a well defined peak load is reached. The footings in sand continue to support about 70% of the peak load up to rotations of about 20° while the footings in the clay with no angle of shear resistance lose load progressively after the peak is reached. The footings tested in soils with both cohesion and an angle of shear resistance had no well defined point of maximum resistance up to rotations of about 20°, but were marked by a very rapid increase in load with increased rotations up to a rotation of about 5°, with a rapid decrease in the slope of the load versus rotation curve for rotations between 5° and 20°. Photographs of the surrounding soil surface for typical tests are shown in Figures 11 through 13.

On the basis of these model tests the load corresponding to a footing rotation of 5° was chosen to use in correlating the theory with test data.

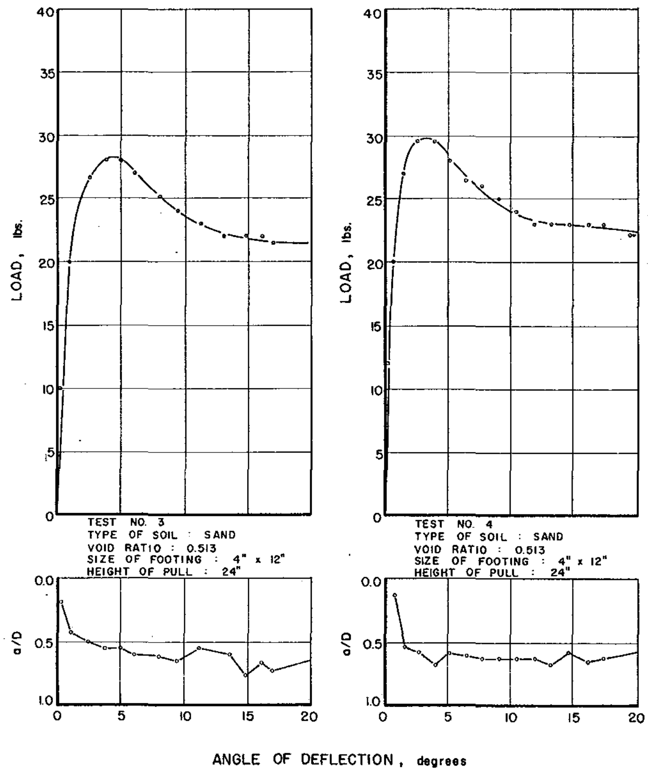

Figure 7. Typical tests in Ottawa Sand.

TABLE 3. RESULTS OF MODEL FOOTING TESTS

Description of Tests				Results of Tests				Soil Parameters		
Test Number	Type of Soil	Size of Footing, d × D, Inches	Height of Pull, H, Inches	Max. Load, P_{max} Lbs.	Defl. @ P_{max}, Deg.	Load, P @ 5°, Lbs.	Pt. of Rotation @ 5°, a/D	c PSF	ϕ Deg.	γ PCF
1	Ottawa Sand	4 × 12*	24	28.3	6° 30′	28.1	0.74		37	109
2	Ottawa Sand	4 × 12	24	34.0	2° 30′	29.0	0.60		37	109
3	Ottawa Sand	4 × 12	24	28.1	4° 30′	28.0	0.55		37	109
4	Ottawa Sand	4 × 12	24	29.7	3° 10′	28.3	0.62		37	109
5	Ottawa Sand	4 × 10	20	20.0					37	109
6	Ottawa Sand	4 × 12	24	33.0	4° 00′	31.0	0.55		37	109
7	Ottawa Sand	4 × 12	24	26.1	3° 40′	25.6	0.63		37	109
8	Ottawa Sand	4 × 12	24			9.3	0.64		32	102
9	Ottawa Sand	4 × 12	24			14.3	0.65		32	102
10	Ottawa Sand	4 × 10	20	22.0	3° 30′	20.8	0.63		37	109
11	Ottawa Sand	4 × 10	20	18.5	2° 50′	16.6	0.62		37	109
12	Ottawa Sand	4 × 10	10	33.5	4° 20′	33.3	0.60		37	109
13	Ottawa Sand	3 × 12	24	22.0	4° 50′	22.0	0.67		37	109
14	Ottawa Sand	3 × 12	12	48.0	4° 40′	48.0	0.58		37	109
15	Ottawa Sand	2 × 12	24			22.3	0.70		37	109
16	Ottawa Sand	4 × 12	12	52.0	4° 10′	51.3	0.63		37	109
17	Ottawa Sand	4 × 12	0	115.0	4° 10′	113.0	0.69		37	109
E-1	Easterwood Clay	4 × 10	20	498.0	7° 40′	488.0	0.46	2810	9	133
E-2	Easterwood Clay	4 × 12	42	410.0	9° 00′	385.0	0.53	2810	9	133
E-3	Easterwood Clay	4 × 12	24			500.0	0.54	2810	9	133
E-4	Easterwood Clay	4 × 12	12			615.0	0.64	2810	9	133
E-5	Easterwood Clay	3 × 12	24	352.0	7° 30′	340.0	0.63	2810	9	133
C-1	Trinity Clay	4 × 10	20	246.0	4° 30′	245.0	0.56	3790		126
C-2	Trinity Clay	4 × 12	24	357.0	6° 20′	348.0	0.68	3790		126
C-3	Trinity Clay	3 × 12	24	290.0	3° 20′	273.0	0.66	3790		126
L-1	33% Trinity Clay 67% Concrete Sand	4 × 12	24			120.0	0.73	794	3.5	123
L-2	67% Trinity Clay 33% Concrete Sand	4 × 12	24			164.0	0.59	1152	5	126
L-3	33% Trinity Clay 67% Concrete Sand	4 × 12	24			238.0	0.63	1411	12	132

*4-inch diameter × 12-inch depth.

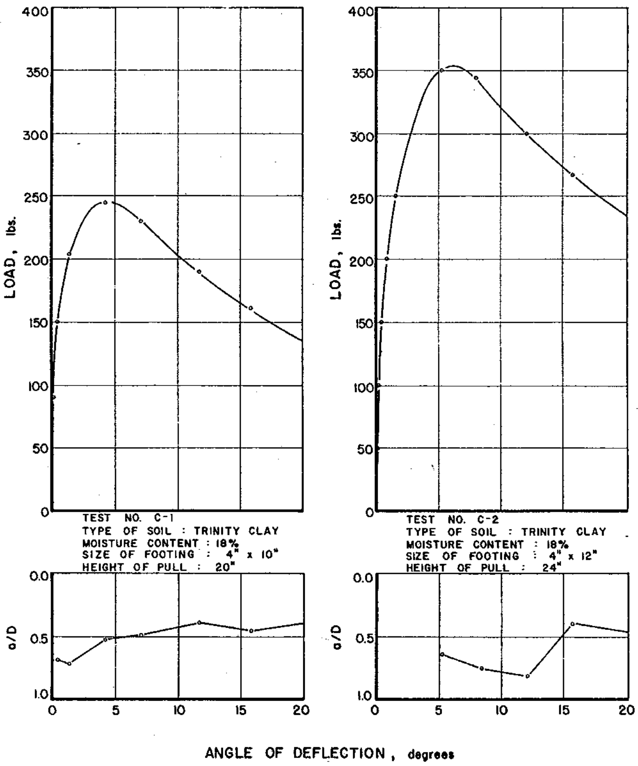

Figure 8. Typical tests in Trinity Clay.

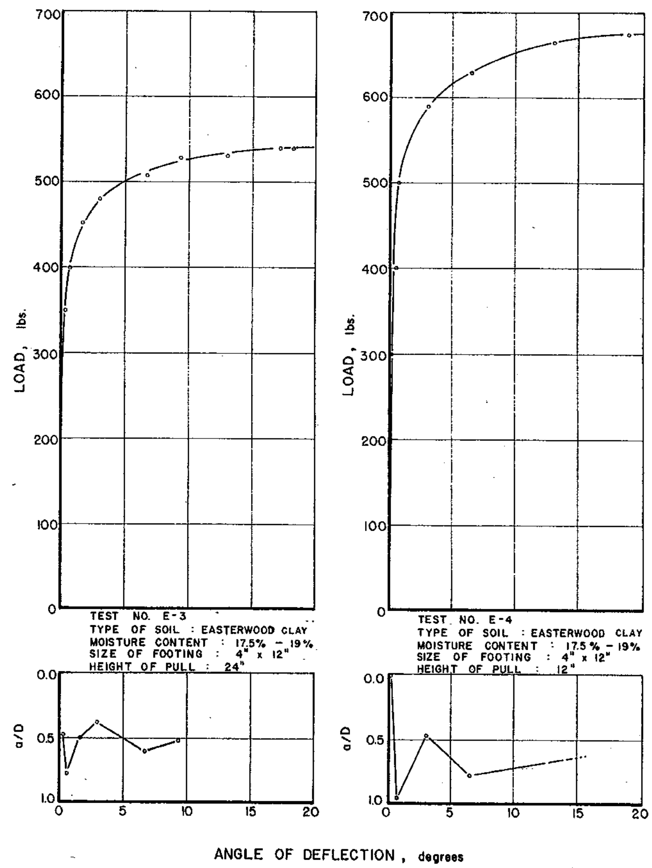

Figure 9. Typical tests in Easterwood Clay.

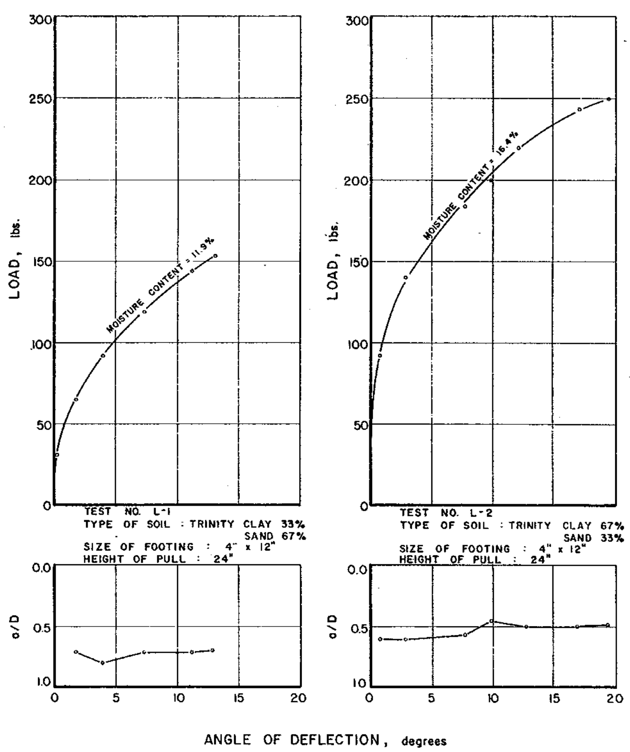

Figure 10. Typical tests in clay-sand mixtures.

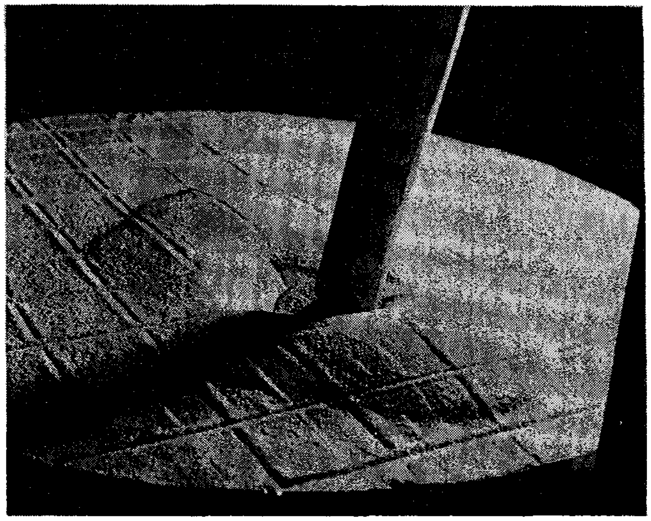

Figure 11. Test of footing in Ottawa Sand.

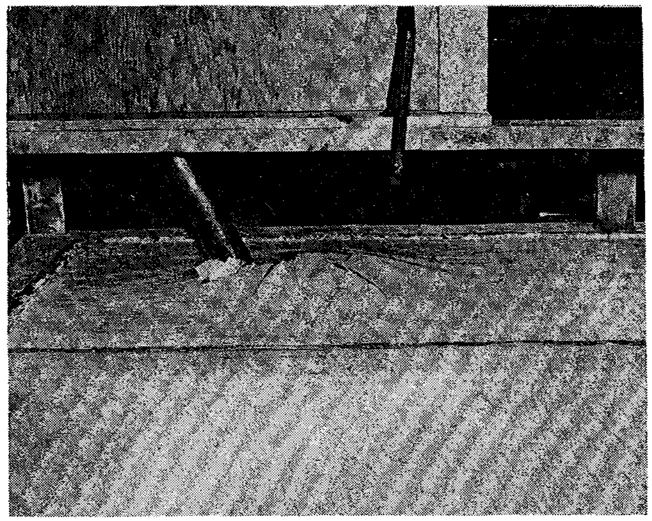

Figure 13. Test of footing in Trinity Clay.

Figure 12. Test of footing in Easterwood Clay.

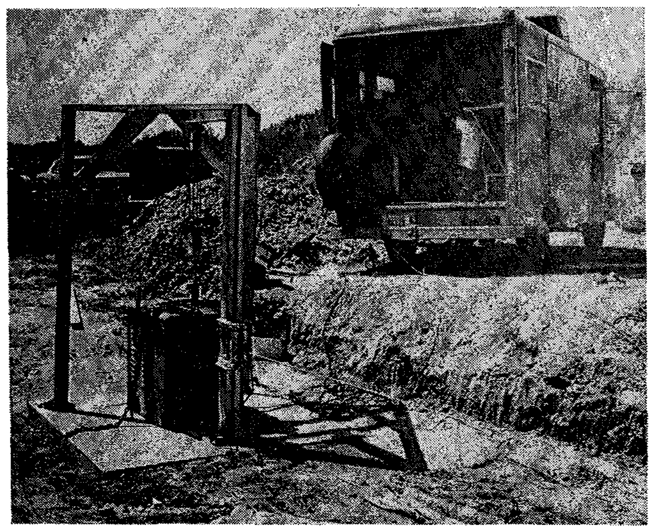

Figure 13a. Test set up at Easterwood.

Comparison of Test Results With Theory

In developing a correlation between the new theory and the model tests reported in this paper, it was necessary to determine the influence of the various coefficients introduced in Research Report 105-1 and to determine the optimum value of these coefficients.

As discussed in 105-1, it was necessary to introduce a modifying factor for the Rankine coefficients of passive and active earth pressure. This factor was designated B., and was applied as follows.

$$K_1 = K_p = B \tan^2 \left(45^\circ + \frac{\phi}{2} \right)$$

$$K_2 = 2B \tan \left(45^\circ + \frac{\phi}{2} \right)$$

$$K_A = B \tan^2 \left(45^\circ - \frac{\phi}{2} \right)$$

An additional coefficient was dictated by analysis of the model tests in Ottawa sands. It was found that predicted values of the footing rotation point were considerably lower than those values observed in the tests. Study of this problem indicated that the soil surrounding the footing was developing higher passive stresses in the direction of the applied load (above the rotation point) and lower soil stresses opposite in direction to the applied load (below the rotation point) than the unmodified theory indicated.

It was surmised that the shearing stresses, acting downward on the soil in front of the advancing face of the footing above the rotation point, produced a slightly greater confining pressure on this soil than would be indicated by the weight of the soil alone. Similarly, the upward shearing stresses on the soil behind the footing below the rotation point act to reduce the effective confining pressure. This change in confining pressure was accounted for by a modification of the effective unit weight of the soil in the following way.

$$\gamma_1 = \gamma\ (1 + k \tan \phi)$$
$$\gamma_2 = \gamma\ (1 - k \tan \phi)$$

Where:

γ_1 = Modified unit weight of soil in the direction of the applied load.

γ_2 = Modified unit weight of soil in the direction opposite the applied load.

k = Unit weight coefficient.

Other coefficients introduced or used in Research Report 105-1 were:

J_1 = Coefficient of shear stress, vertical footing surfaces.

J_2 = Coefficient of shear stress, footing bottom.

K_0 = Coefficient of earth pressure at rest.

The influence of these coefficients on the predicted load and the point of rotation was determined by allowing each to vary while the others were held constant. Typical sets of curves developed in this manner are shown in Figures 14, 15, and 16.

Figure 14, representing a cohesionless material such as the dry Ottawa sand, shows that two coefficients have a high influence on the theoretical solution. The unit weight coefficient, k, has a high degree of influence on the predicted position of the point of rotation. The earth pressure coefficient modifier, B, has a great influence on the predicted load.

In Figures 15 and 16, which represent soils with cohesion only and soils with both cohesion and an angle of shear resistance, respectively, the great influence of B is again shown, while k is no longer very influential.

A study of coefficient sensitivity charts and comparison of predicted and observed loads indicated that all coefficients except B could be held constant for the range of soils tested in this program. The values set for these coefficients are:

$$J_1 = J_2 = 0.7$$
$$K_0 = 0.5$$
$$k = 0.5$$

It was found that the value of B necessary to successfully predict ultimate loads varied with the soil parameters of cohesion (c) and angle of internal friction (ϕ). The average values of B indicated by the tests on Ottawa sand, Easterwood clay, laboratory clay-sand mixtures, and Trinity clay were used to develop a prediction equation for B. This equation was determined from the function of ϕ used in the theoretical solution and a linear model in terms of c. This prediction equation is given and presented in graphical form in Figure 17.

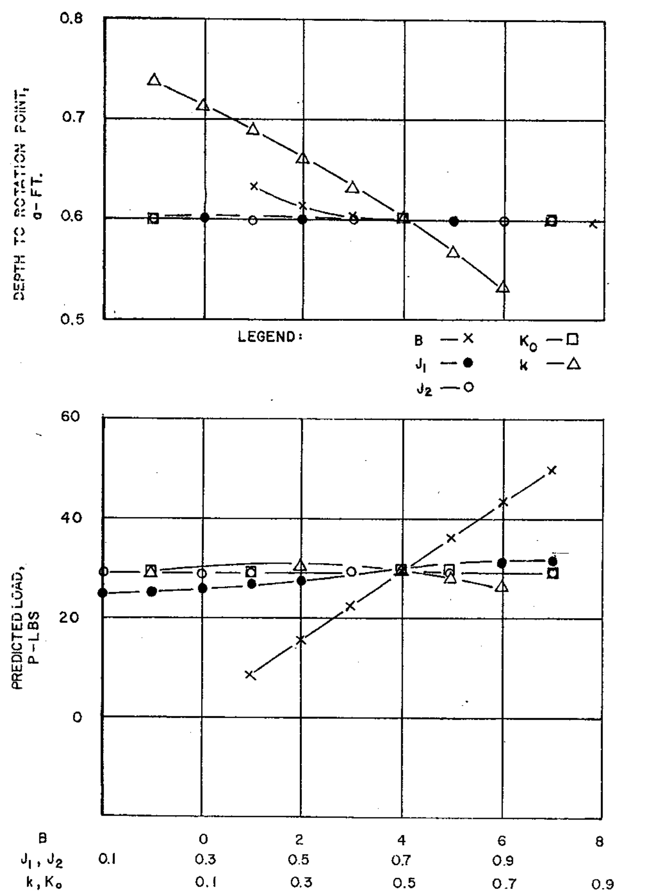

Figure 14. Coefficient sensitivity, c=0 psf, ϕ=37°, H=2 ft., D=1 ft., d=0.33 ft.

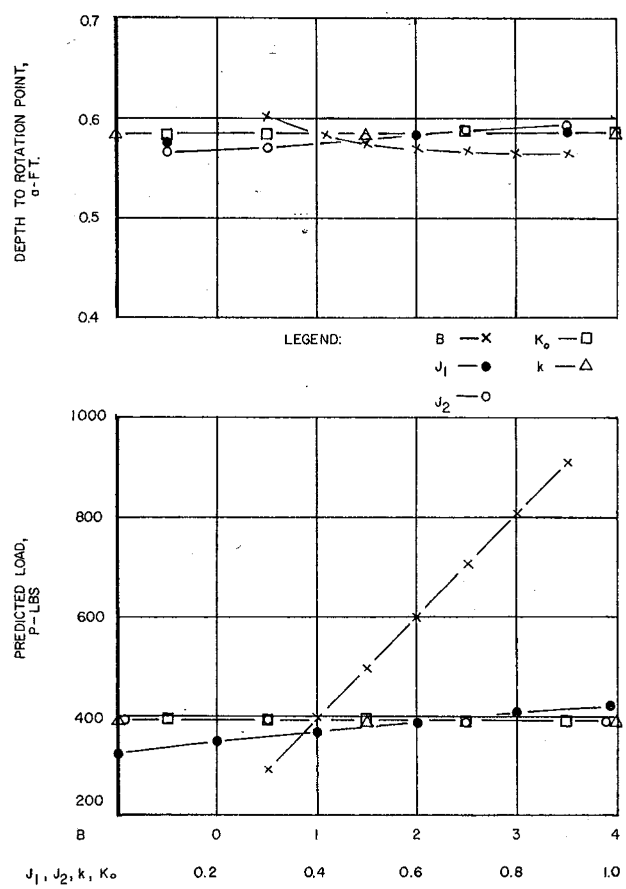

Figure 15. Coefficient sensitivity, c=3900 psf, ϕ=0°, H=2 ft., D=1 ft., d=0.33 ft.

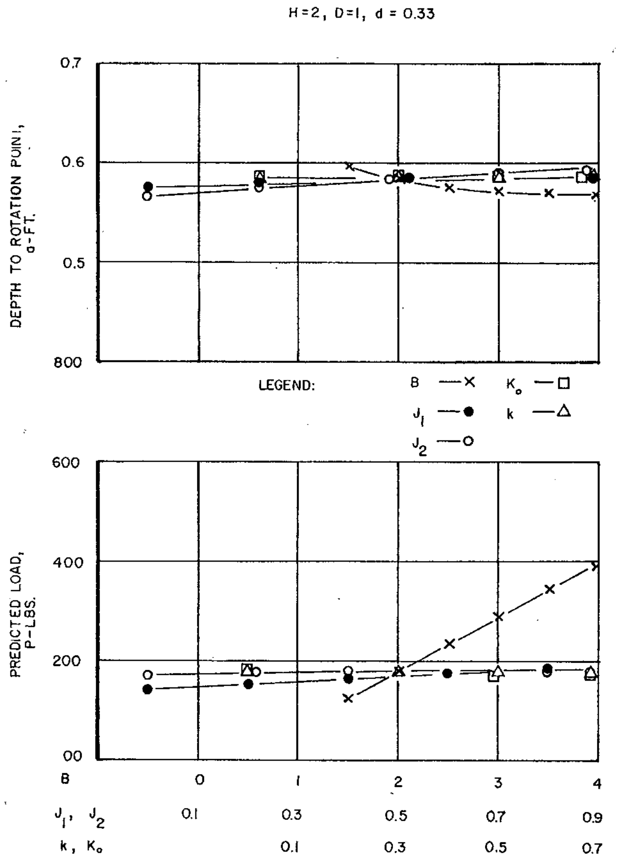

Figure 16. Coefficient sensitivity, $c=1140$ psf, $\phi=12°$, $H=2$ ft., $D=1$ ft., $d=0.33$ ft.

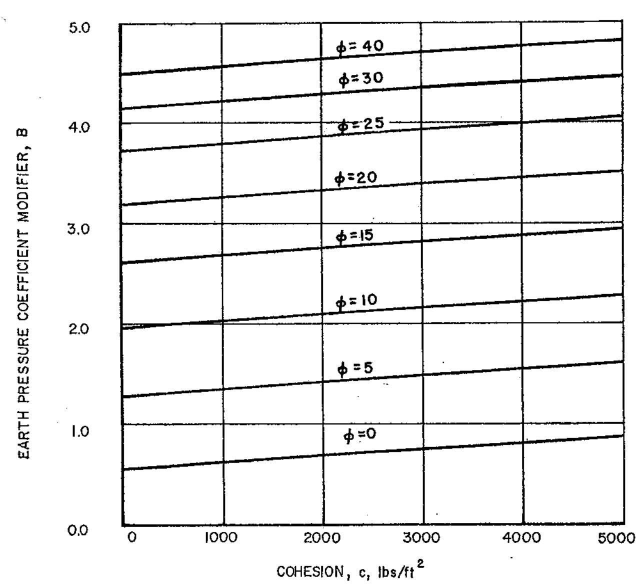

B EQUATION

$$B = 0.0000673\,c + 10.25\tan\phi + 2.686\tan(45+\phi/2) - 2.141\tan^2(45+\phi/2)$$

Figure 17. Solution for earth pressure coefficient modifier.

TABLE 4. COMPARISON OF TEST RESULTS WITH THEORY, COHESIVE SOILS

Test No.	(1) Load at Rotation of 5° (1) lbs.	(2) Predicted Loads: Conventional Theory[7] (2) lbs.	(3) Predicted Loads: New Theory[1] (3) lbs.	(4) Test Load to Predicted Load Ratios (1)/(2)	(5) Test Load to Predicted Load Ratios (1)/(3)
E-1	488	200	459	2.44	1.06
E-2	385	179	337	2.15	1.14
E-3	500	241	535	2.07	.935
E-4	615	337	871	1.82	.706
E-5	340	181	384	1.88	.885
C-1	245	230	300	1.07	.817
C-2	348	276	344	1.26	1.01
C-3	273	207	241	1.32	1.13
L-1	120	63	92	1.90	1.30
L-2	164	93	154	1.76	1.06
L-3	238	128	324	1.86	.735

Using these coefficients in the theoretical solution resulted in the comparison of predicted loads and test loads shown in Tables 4 and 5. Also included in these tables are values of loads predicted using the old theory.

In column (4) of Tables 4 and 5 the ratio of each test load to the corresponding load predicted by the conventional theory[7] is tabulated. The test loads vary from an average of 20% higher than predicted loads for the Trinity clay, to about 500% higher for the Ottawa sand. For all 28 tests (seven different soil conditions) the test values average 4.09 times greater than the loads predicted by the conventional theory. Thus, the test loads are about 300% higher than the predicted loads.

Tables 4 and 5 also present a comparison between the test loads and the new theory in column (5). The ratio of test loads to predicted loads shown in column (5) are about the same for each different type of soil.

Two rather low values of this ratio (.410 and .630) are given by tests S8 and S9. These were tests in Ottawa sand which was in a very loose condition. Apparently, the new theory gives a rather poor estimate of the ultimate load for footings in a very loose sandy soil. Fortunately, this is not often a condition of practical importance.

Another test which correlated poorly was S15. This was an extremely slender footing, with a ratio of footing width to depth of 0.167. The test load was 50% higher than the predicted load, an error on the conservative side.

The average value of the test load to predicted load ratio was 0.912 for all footings tested. The new theory thus predicted loads that averaged 10% higher than the test loads.

The reliability of the theory with variation in the geometry of the footing tests (i.e. variation in H/D and d/D) is shown by Figures 18 through 20. Of the 20 test points compared to theoretical curves in these figures, only three show considerable divergence from the theoretical curves. The test point at a value of H/D of 1.0 in Figure 18 is about 30% low and the first and third points in Figure 20 are 18% high and 13% low, respectively. With these possible exceptions, the test data points closely followed the theoretical curves.

TABLE 5. COMPARISON OF TEST RESULTS WITH THEORY, OTTAWA SAND

Test No.	(1) Load at Rotation of 5°	(2) Predicted Loads: Conventional Theory[7]	(3) Predicted Loads: New Theory[1]	(4) Test Load to Predicted Load Ratios	(5) Test Load to Predicted Load Ratios
	(1) lbs.	(2) lbs.	(3) lbs.	(1)/(2)	(1)/(3)
S1	28.1	5.47	32.5	5.14	.865
S2	29.0	5.47	32.5	5.30	.892
S3	28.0	5.47	32.5	5.12	.862
S4	28.3	5.47	32.5	5.17	.871
S5	20.0	3.79	23.9	5.28	.837
S6	31.0	5.47	32.5	5.67	.954
S7	25.6	3.47	32.5	4.68	.788
S8	9.3	3.83	22.7	2.43	.410
S9	14.3	3.83	22.7	3.73	.630
S10	20.8	3.79	23.9	5.49	.870
S11	16.6	3.79	23.9	4.38	.695
S12	33.3	5.30	38.2	6.28	.872
S13	22.0	4.11	23.3	5.35	.944
S14	48.0	5.74	50.8	8.36	.945
S15	22.3	2.75	14.9	8.11	1.50
S16	51.3	7.64	52.5	6.71	.977
S17	113.0	14.7	134.0	7.69	.843
			Average	4.09	.912
			Range	1.07-8.36	.410-1.50
			C.V.	55%	23%

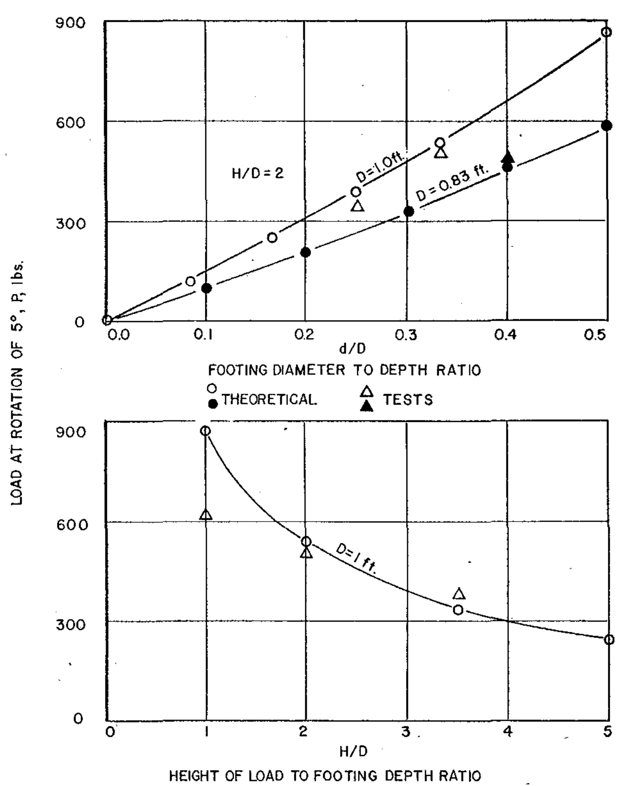

Figure 18. Easterwood Clay tests.

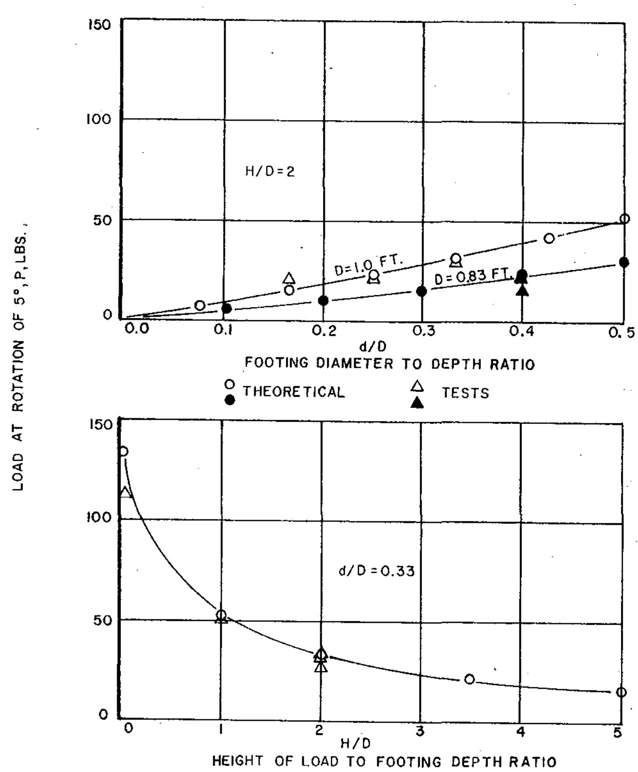

Figure 19. Ottawa Sand tests.

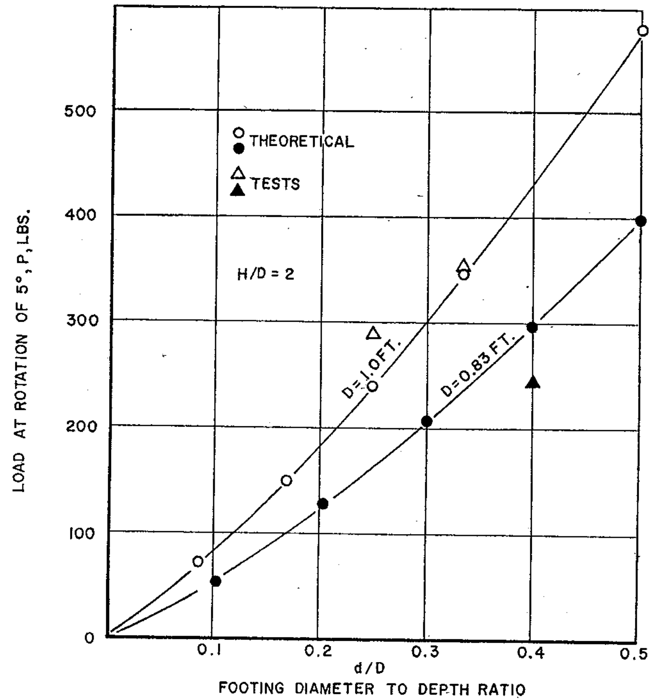

Figure 20. Trinity Clay tests.

Summary

The purpose of the model tests reported in this paper was to determine if the theory developed in Research Report 105-1 could be successfully used to predict the ultimate lateral loads which could be resisted by drilled shaft footings.

The various coefficients involved in the theoretical solution have been evaluated by correlation of the theory with the model tests. Based on this correlation the theory can predict, with reasonable accuracy, the ultimate loads on footing models in soils ranging from cohesionless sand to clays.

The indication given by these model tests is that the conventional design techniques for service structure footings are extremely conservative, and that existing footings are overdesigned by a large margin.

The next step in determining the value of the new theory can predict, with reasonable accuracy, the ultiings are presently under construction as part of Research Study 2-5-66-105.

Selected References

1. Ivey, Don L., "Theory, Resistance of a Drilled Shaft Footing to Overturning Loads," Research Report No. 105-1, Texas Transportation Institute, August, 1967.
2. Lambe, William T., *Soil Testing for Engineers,* John Wiley & Sons, Inc., 1951.
3. Taylor, Donald W., *Fundamentals of Soil Mechanics,* John Wiley & Sons, Inc., 1948.
4. Seed, H. B. and Chan, C. K., "Thixotropic Characteristics of Compacted Clay," *Proceedings, ASCE,* Vol. 83, S.M. 4, November, 1957.
5. Mitchell, J. K., "Fundamental Aspects of Thixotropy in Soils," *Proceedings, ASCE,* Vol. 86, S.M. 3, June, 1960.
6. Moretto, O., "Effects of Natural Hardening on the Unconfined Compression Strength of Remolded Clays," Second International Conference on Soil Mechanics and Foundation Engineering, Rotterdam, Vol. 1, 1948.
7. Ivey, Don L., and Hawkins, Leon, "Signboard Footings to Resist Wind Loads," *Civil Engineering,* December, 1966, p. 34.

Appendix

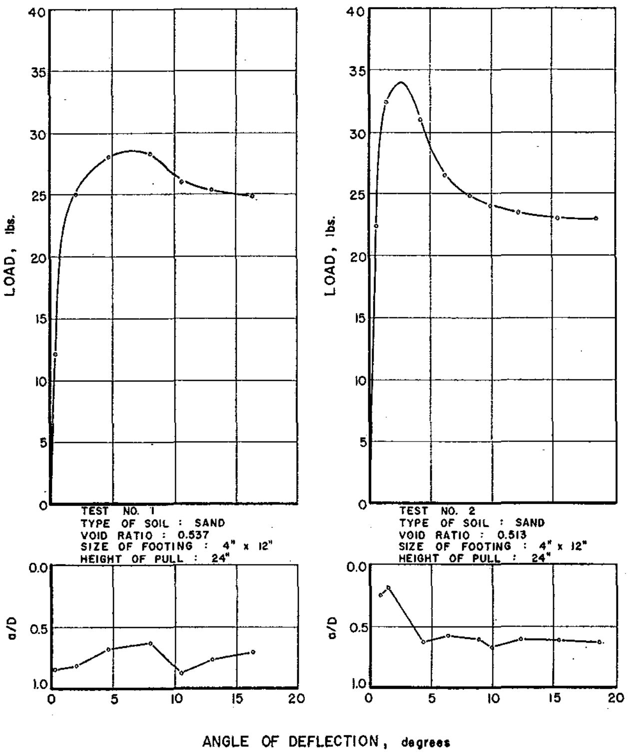

AN ATTEMPT WAS MADE TO PHOTOGRAPH THE PROGRESS OF THIS TEST. LIGHT PRODUCED BY THE FLASH ATTACHMENT CAUSED OVER EXPOSURE OF THE RECORDING PAPER. DUE TO THIS THE RECORD OF DEFLECTIONS WAS DESTROYED.

(MAXIMUM LOAD = 20 LBS.)

TEST NO. 5
TYPE OF SOIL : SAND
VOID RATIO : 0.511
SIZE OF FOOTING : 4" x 10"
HEIGHT OF PULL : 20"

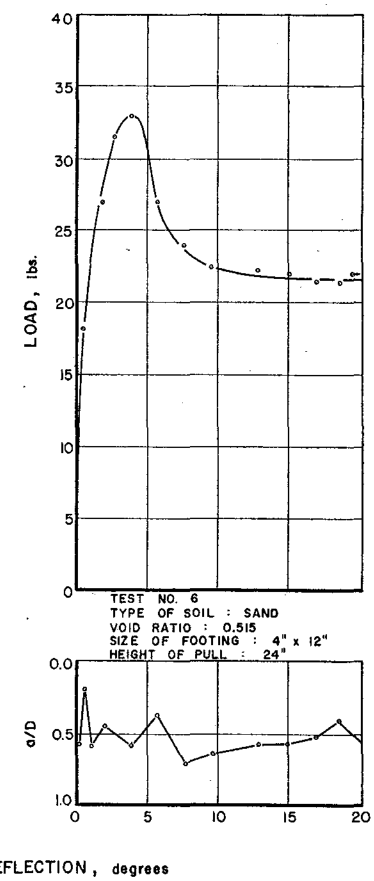

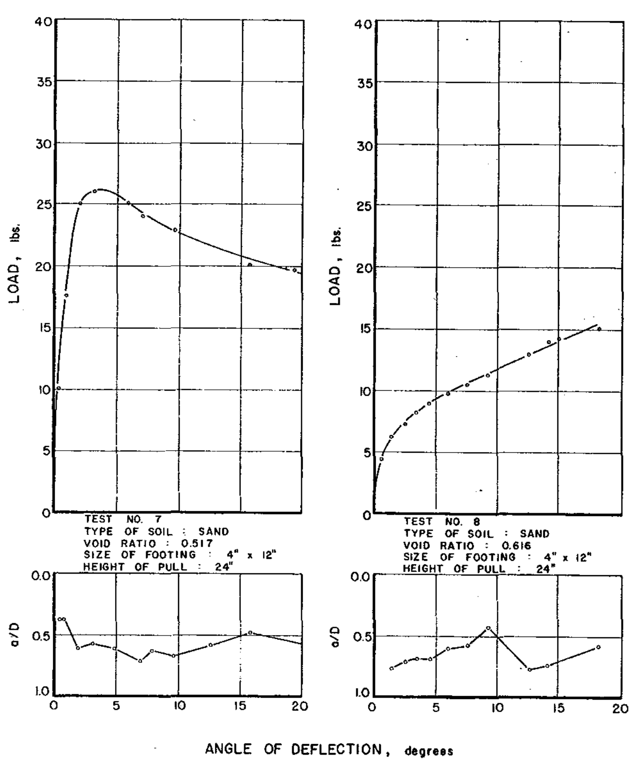

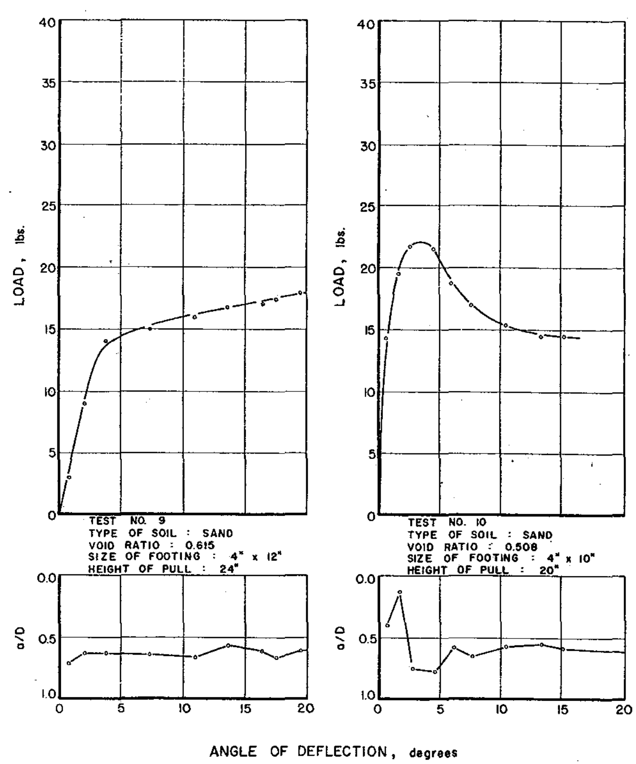

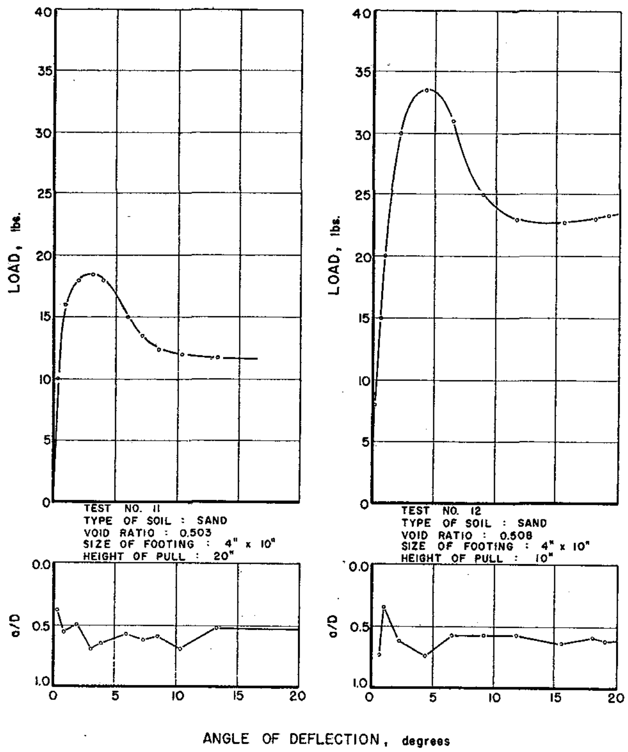
LOAD, lbs.
TEST NO. 11
TYPE OF SOIL : SAND
VOID RATIO : 0.503
SIZE OF FOOTING : 4" x 10"
HEIGHT OF PULL : 20"
TEST NO. 12
TYPE OF SOIL : SAND
VOID RATIO : 0.508
SIZE OF FOOTING : 4" x 10"
HEIGHT OF PULL : 10"
a/D
ANGLE OF DEFLECTION, degrees

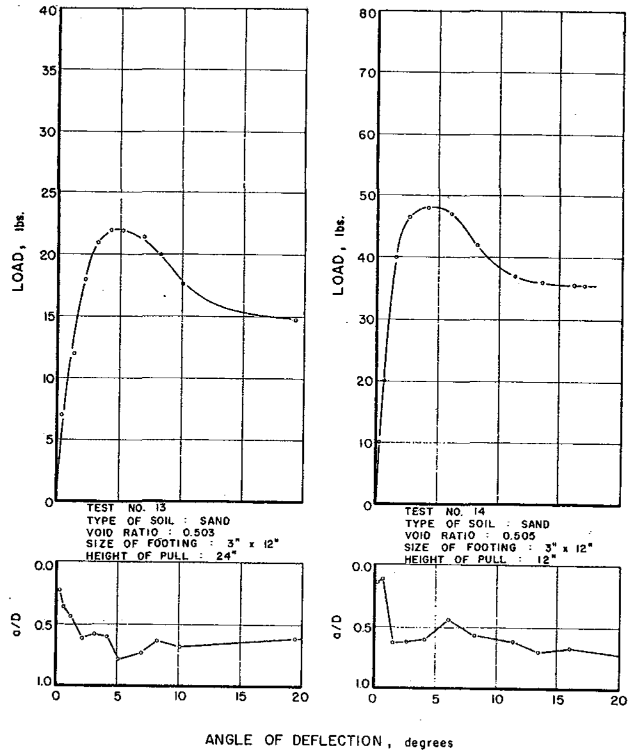
LOAD, lbs.
TEST NO. 13
TYPE OF SOIL : SAND
VOID RATIO : 0.503
SIZE OF FOOTING : 3" x 12"
HEIGHT OF PULL : 24"
TEST NO. 14
TYPE OF SOIL : SAND
VOID RATIO : 0.505
SIZE OF FOOTING : 3" x 12"
HEIGHT OF PULL : 12"
a/D
ANGLE OF DEFLECTION, degrees

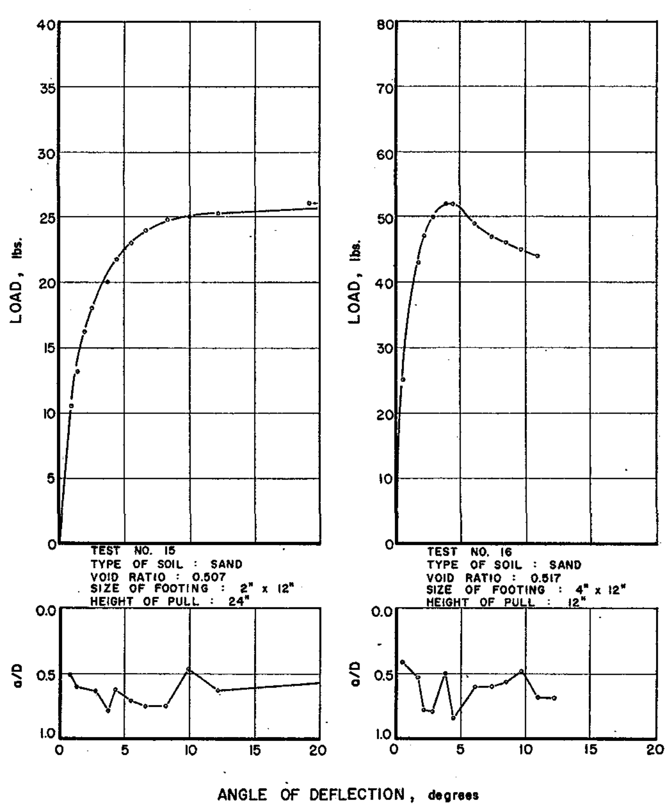
LOAD, lbs.
TEST NO. 15
TYPE OF SOIL : SAND
VOID RATIO : 0.507
SIZE OF FOOTING : 2" x 12"
HEIGHT OF PULL : 24"
TEST NO. 16
TYPE OF SOIL : SAND
VOID RATIO : 0.517
SIZE OF FOOTING : 4" x 12"
HEIGHT OF PULL : 12"
a/D
ANGLE OF DEFLECTION, degrees

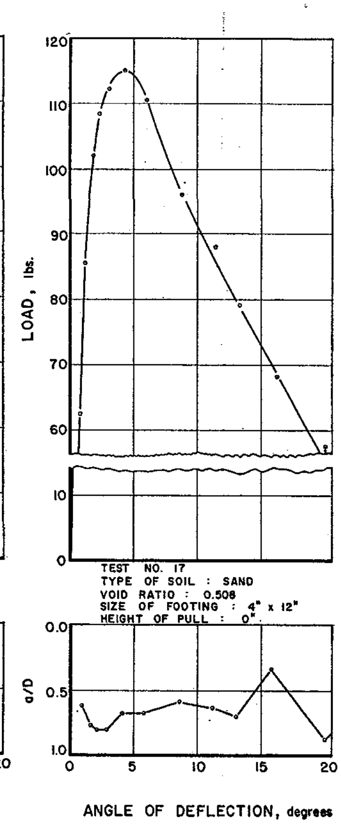
LOAD, lbs.
TEST NO. 17
TYPE OF SOIL : SAND
VOID RATIO : 0.508
SIZE OF FOOTING : 4" x 12"
HEIGHT OF PULL : 0"
a/D
ANGLE OF DEFLECTION, degrees

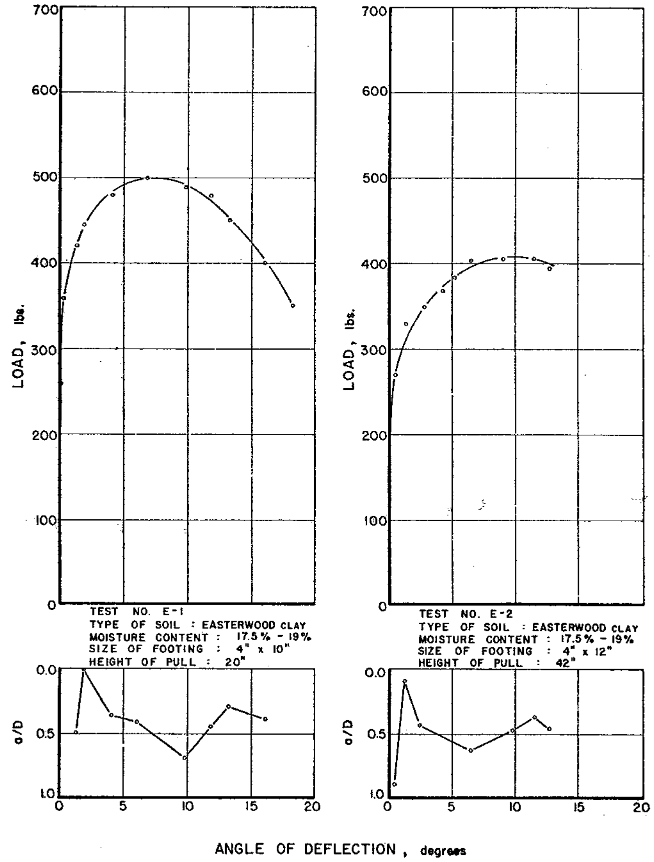
LOAD, lbs.
TEST NO. E-1
TYPE OF SOIL : EASTERWOOD CLAY
MOISTURE CONTENT : 17.5% - 19%
SIZE OF FOOTING : 4" x 10"
HEIGHT OF PULL : 20"
a/D
TEST NO. E-2
TYPE OF SOIL : EASTERWOOD CLAY
MOISTURE CONTENT : 17.5% - 19%
SIZE OF FOOTING : 4" x 12"
HEIGHT OF PULL : 42"
ANGLE OF DEFLECTION, degrees

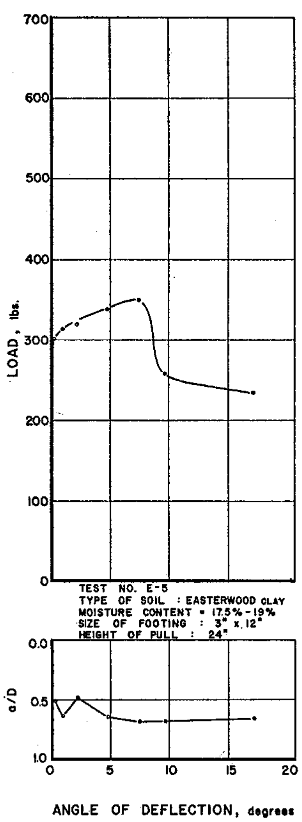
LOAD, lbs.
TEST NO. E-5
TYPE OF SOIL : EASTERWOOD CLAY
MOISTURE CONTENT = 17.5%-19%
SIZE OF FOOTING : 3" x 12"
HEIGHT OF PULL : 24"
a/D
ANGLE OF DEFLECTION, degrees

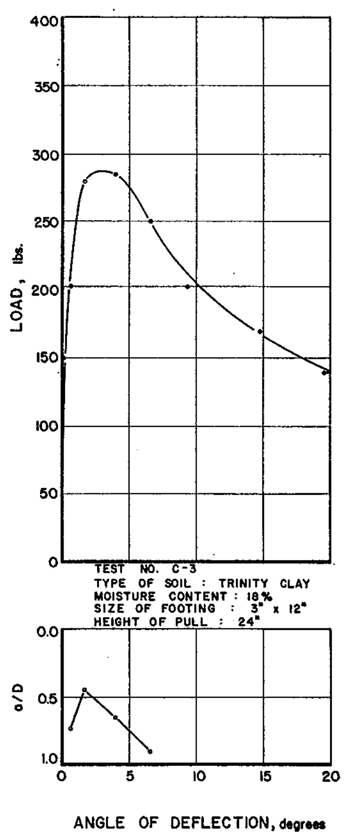
LOAD, lbs.
TEST NO. C-3
TYPE OF SOIL : TRINITY CLAY
MOISTURE CONTENT : 18%
SIZE OF FOOTING : 3" x 12"
HEIGHT OF PULL : 24"
a/D
ANGLE OF DEFLECTION, degrees

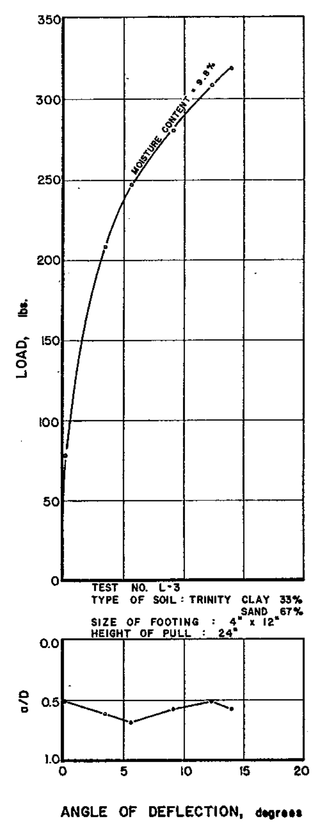
LOAD, lbs.
MOISTURE CONTENT = 9.5%
TEST NO. L-3
TYPE OF SOIL : TRINITY CLAY 33% SAND 67%
SIZE OF FOOTING : 4" x 12"
HEIGHT OF PULL : 24"
a/D
ANGLE OF DEFLECTION, degrees